Scientia Iranica B (2023) 30(1), 52–63

Sharif University of Technology
Scientia Iranica
Transactions B: Mechanical Engineering
http://scientiairanica.sharif.edu

Research Note

A combined approach to grey relational analysis and principal component analysis for development of input parameters in the wear characterization of Al7075 ($SiC+Al_2O_3$) hybrid metal matrix composites

S. Selvarasu* **and L. Jayakumar**

Department of Mechanical Engineering, Arunai Engineering College, Tiruvannamalai, Tamil Nadu, India.

Received 18 April 2021; received in revised form 24 September 2021; accepted 19 September 2022

KEYWORDS
Al7075;
SiC;
Al_2O_3;
AHMMCs;
Stir casting;
DoE;
Mechanical properties;
GRA;
PCA.

Abstract. The current research aims to study the effect of mechanical stir casting on the Al7075-based lightweight alloy made of Al_2O_3 and SiC at different times and speeds of the stirrer. As observed, the hybrid metal matrix improved the wear resistance of the composite material Al7075 ($SiC+Al_2O_3$). Experimental designs were formulated using Taguchi's DoE and based on four levels and four parameters, L_{16} OA was selected. Both Grey Relational Analysis (GRA) and Principle Component Analysis (PCA) were employed to calculate the matrix composition. In addition, Pin-On-Disc (POD) test was done to measure the wear resistance of the cast pins. Further, mechanical characterizations such as tensile, hardness, impact, density, and porosity were identified through testing. The optimum parameters in this study were SiC of 6%, Al_2O_3 of 4%, stirrer time of 15 min, and stirrer speed of 600 rpm, which led to the low wear loss of 0.0034 g, superior micro hardness of 154.22 BHN, tensile strength of 443.61 MPa, and impact energy of 3 J. From the ANOVA results, the stirrer speed was the most influential parameter among others with the share of 49.40%. The worn surfaces were identified through the Scanning Electron Microscope (SEM) and Energy Dispersive X-ray (EDX) analyses.

1. Introduction

In recent years, the application of 7075-based aluminum alloys as designing materials in different industries such as aerospace, vehicles, and marine industries has given preference owing to their physical and thermal properties. There are different grades of aluminum alloys available in the market among which Al7075 grade alloy is recognized as the best one due to its high resistance to corrosion, qualitative grade, admirable strength, and wide applicability to automotive sector, structuring, and commercial fields [1]. The wear performance of the components of all moving parts was evaluated in a direct contact manner. These components are regularly lubricated to accomplish the frictional process. Performing the intended operation, especially on the size and shape of the component, is impossible. Of note, the worn-out components can cause an increase in the operating cost and mechanism working time. Hybrid metal composites are mostly preferred to

*. *Corresponding author. Tel.: +91-8489614900*
E-mail addresses: selvarasu2007@gmail.com (S. Selvarasu); jkpathy@gmail.com (L. Jayakumar)

doi: 10.24200/sci.2022.58141.5586

Table 1. Composition of Al7075.

Si	Fe	Cu	Mn	Mg	Cr	Ni	Zn	Pb	Ti	Al
0.15	0.2	2.8	0.03	1.91	0.005	0.203	4.264	0.001	0.008	Bal.

the metal alloys with more degrees of reinforcement, hence being widely used. Aluminum Hybrid Metal Matrix Composites (AHMMCs) of the particulate are found in many applications. Several researchers stated that the rate of changes in different parameters would significantly affect the wear performance behavior [2,3].

Once used, composite materials can affect the rate of development in engineering applications, and AHMMCs are generally reinforced with other metal, ceramic, and organic compounds. Such reinforcement would, in turn, improve the mechanical properties such as tensile strength, hardness, solidity, and low firmness. The wear performance was compared to the reference metal performance in terms of quality [4]. AHMMCs increased the inclination to fabricate composites at low costs in many fields such as automobile, airplane, aerospace, and other supplementary fields. The alloy composed of SiC, Al_2O_3, and graphite reinforcement has good compressive power and wear resistance [5].

In recent years, enormous studies have attempted to fabricate metal composites, and a stir casting process has been proposed, which is an economically easy composite fabrication method [6,7]. As a result, AHMMCs that are characterized by good wear resistance, high specific strength, and high structural efficiency as well as several good electrical and thermal properties with low density are prepared using two or more different types of metal alloys [8]. Stir casting process enjoys several advantages: flexibility, plainness, and volume production. The determining variables here are the concentration, temperatures, types of wettability agents, stirring methods, and stirring time of the reinforcement materials [9,10].

Statistical tools were used for optimization of AHMMC materials casting wear properties. In addition, Taguchi optimization approach was used for single-variable optimization to fulfill the quality attributes. GRA-PCA-based Taguchi optimization was applied for multi-variable optimization. In this study, the Taguchi strategy experimental run was drafted on an orthogonal array [11,12] where the Aluminum grade 7075 was used as the matrix material.

The main objective of this research work is to improve the wear quality and mechanical properties of alloy Al7075 with silicon carbide (SiC) and aluminum oxide (Al_2O_3). To this end, AHMMCs are cast through the stir casting process with varying compositions, stirrer times, and stirrer speeds. Then, the optimum parameters were optimized for the Al7075. The wear properties of the cast material were analyzed by Pin-On-Disc (POD) wear testing. In addition, the composite properties such as the density, tensile, hardness, and porosity were characterized through different tests. Further, Scanning Electron Microscope (SEM) and Energy Dispersive X-ray (EDX) analysis was employed to investigate the worn surfaces.

2. Selection of materials

2.1. Matrix and reinforcement material

Various composite materials were developed using different matrix types as well as the size and shape of the reinforcement material depending on their applications. The good properties of the composite are obtained through uniform distribution and optimization [13,14].

The functionalized AHMMCs exhibited specific power and adherence at both room and raised temperatures. These composites are the best materials for structural applications because of their low density and low cost. Aluminum grade 7075 material was used as the matrix material in this study. Table 1 shows the composition of Al7075.

Ceramic materials are generally employed to reinforce aluminum alloys like TiC, SiC, Si_3N_4, TiB_2, ZrB_2, Al_2O_3, SiO_2, and AlN. Generally, SiC is used in many applications in factories producing abrasives and ceramics with the wear-resistant applications. Aluminum (Al_2O_3) is also commonly used in the production of respective metals, ceramics, refractories, etc. which is abrasive in nature due to its hardness properties. In this study, silicon carbide (SiC)-100 μm and aluminum oxide (Al_2O_3)-100 μm were used as the reinforcement materials.

2.2. Fabrication of AHMMCs

In the current investigation, 100 μm particles (SiC+Al_2O_3) were used with Al7075. The process of melting was carried out using coke furnace according to the given instructions given in the traditional procedure, as shown in Figure 1. The reinforcement materials were pre-heated at 400°C temperature for 30 min and, then, mixed with a molten base metal with mechanically continuous stirring for uniform dispersion, as shown in Table 2 [15]. During the stir casting, 1% of magnesium was slowly added to increase the alloy reinforcements and then, the molten metal alloy was poured into die to form the cast specimens of 25 mm in diameter and 150 mm in length. The compositions of Al_2O_3, SiC, and stirrer time and speed for each specimen were chosen from Table 2.

Figure 1. Stir casting setup.

Table 2. Input parameter and levels.

Parameters	Symbol	Levels			
		1	2	3	4
SiC	A	3	6	9	12
Al_2O_3	B	2	4	6	8
Stirrer time (min)	C	5	10	15	20
Stirrer speed (rpm)	D	500	600	700	800

3. Experimental design

3.1. Plan of Experiments (DoE)

Taguchi's statistical method effectively elaborates on the impacts of the process parameters. In other words, the effects of each individual factor can be optimized through this method. In addition, this method can predict the best experimental design among other available designs for an engineering problem. In this study, it further developed an orthogonal array to analyze the responses based on the least number of experimental trials [16].

Table 2 lists four input parameters (SiC, Al_2O_3, stirrer time, and stirrer speed) with four levels at this Taguchi's DoE [17]. Minitab 19 statistical package with L_{16} OA was also used for optimization of control parameters at different levels given in this table.

3.2. Grey Relational Analysis (GRA)

A multivariate methodology used for GRA of the given input parameters succeeded in determining the optimal parametric conditions. The efficiency of any complex optimization problems could be assessed based on the available limited knowledge [18,19]. To overcome this limitation, GRA evaluated a grade (GRG) for simultaneous assessment of more than one output and to this end, GRA data pre-processing used normalized values. If we need the information for the-lower-the-better, the original sequence will be normalizing, as shown in Eq. (1):

$$\chi_i^*(k) = \frac{\max x_i^0(k) - x_i^0(k)}{\max x_i^0(k) - \min x_i^0(k)}, \tag{1}$$

where $x_i^0(k)$ is the original sequence of the composite data, $x_i^*(k)$ the after-composite data preprocessing, $\max x_i^0(k)$ the highest value of $x_i^0(k)$, and $\min x_i^0(k)$ the smallest value of $x_i^0(k)$. The reference sequence is measured, followed by the normalizing process by scaling the output range between zero and one. In case the data value is closer to 1, due to its greater demand for information, it is considered as the best answer. Finally, Grey Relational Coefficient (GRC) is calculated as a relationship between the ideal and actual values of the experimental results given in Eq. (2):

$$\varsigma_i(k) = \frac{\Delta\min + \varsigma \cdot \Delta\max}{\Delta_{oi}(k) - \varsigma \cdot \Delta\max}, \tag{2}$$

where $\Delta_{oi}(k)$, the deviation sequence, is given in Eq. (3):

$$\Delta_{0i}(k) = \left\| x_o^*(k) - x_i^*(k) \right\|,$$

$$\Delta\max = \max_{\forall j \varepsilon i} \max_{\forall k} \left\| x_0^*(k) - x_i^*(k) \right\|,$$

$$\Delta\min = \min_{\forall j \varepsilon i} \min_{\forall k} \left\| x_0^*(k) - x_i^*(k) \right\|. \tag{3}$$

In Eq. (4), ς is known as an identifying coefficient where $\varsigma_{\varepsilon[0,1]}$, $\varsigma_{=0.5}$ are used normally. In the following, GRG is calculated by taking the average of all the output responses of the GRC given by:

$$y_i = \frac{1}{n} \sum_{k=1i}^{n} \varsigma_i(k). \tag{4}$$

3.3. Principal Component Analysis (PCA)

PCA was first developed by Pearson and Hotelling and it defines the construction based on the linear integration of variance and covariance of all output characteristics [20,21]. The PCA steps are given as follows:

1. To construct the original multi-performance array, the following formula is proposed:

$$x_i(j), i = 1 \quad \text{to} \quad m, j = 1,$$

$$\begin{bmatrix} X_1(1) & X_1(2) & \cdots & \cdots & X_1(n) \\ X_1(1) & X_1(2) & \cdots & \cdots & X_2(n) \\ \cdots & \cdots & \cdots & \cdots & \cdots \\ \cdots & \cdots & \cdots & \cdots & \cdots \\ X_m(1) & X_m(2) & \cdots & \cdots & X_1(n) \end{bmatrix}, \tag{5}$$

   where m denotes the number of experimental runs, and n the number of output or response characteristics. The GRC of each output characteristic is represented by X in this analysis. Here, $n = 2$ and $m = 18$.

2. The correlation coefficient array is evaluated by the following equation:

Figure 2. Pin on disc wear tester.

$$R_{ji} = \frac{Cov(x_i(j), x_i(l)}{\sigma_{xi}(j)x\sigma(l)};$$

$$j = 1 \text{ to } n \quad \text{and} \quad l = 1 \text{ to } n. \tag{6}$$

In Eq. (6), $Cov(x_i(j), x_i(l)$, in the CS stand for $x_i(j)$, $x_i(l)$, respectively, $\sigma_{xi}(j)$ is the Standard deviation of sequence $x!(j)$, and $\sigma_{xi}(j)$ denotes the Standard deviation $x_i(j)$.

3. The correlation coefficient array is used for evaluating eigenvalues and eigenvectors:

$$(R - \lambda_k l_m)\, v_{ik} = 0. \tag{7}$$

In Eq. (7) λ_k denotes eigenvalues; $\sum_{k=1}^{n} \lambda_k n, k = 1, 2, 3, \cdots, n : v_{ik} = (a_{k1}a_{k2}, \cdots, a_{kn})^T$ eigenvectors of the eigenvalue correspond to λ_k.

4. Finally, the principal components are determined using the following equation:

$$y_{mk} = \sum_{i}^{n} x_m(i) * v_{ik}. \tag{8}$$

In Eq. (8), y_{m1} is produced as the first PC, y_{m2} as the second principal component, and so on.

Through the GRA-PCA method the process parameters can be evaluated as follows:

1. The output values are calculated from the POD experiments;
2. Based on the GRA, the normalizing sequence, deviation sequence, and grey relational coefficient are determined in Eqs. (2) and (3);
3. Followed by determining the eigenvector value, the multiplication of GRC can be obtained. In addition, through the PCA, the response performance index can be calculated;
4. The optimal input parameter levels are then obtained;
5. ANOVA finds the determining parameters;
6. Finally, the confirmation test is done.

3.4. Experimental work

The applied load, sliding velocity, and sliding distance of 30 N, 3 m/s, and 2000 m, respectively, were constantly used in the POD wear test. Sixteen pins of 6 mm in diameter and 25 mm in length in the specimens are cast as per L_{16} OA and machined as per dimension. High carbon and high chromium steel 55 mm die and a disc with the thickness of 10 mm were utilized as counter surface materials as per ASTM G99 standard. Figure 2 shows the POD wear tester that explains the surface interactions of the deformed material surface. Tribometer measured the wear between two surfaces in contact and tribological quantities such as frictional force [22,23].

4. Results & discussion

Followed by preparing the pins, the mechanical properties such as density, micro hardness, porosity, and tensile test were analyzed. Then, optimization studies were conducted to identify the most influencing parameter to improve the wear resistance.

4.1. Dry sliding wear studies

The L_{16} orthogonal array in Taguchi method was identified through experimental runs. For this purpose, separate work pins were considered for all levels during investigation. Table 3 shows the measured responses (wear loss and frictional force) for the AHMMCs. Of note, the second experiments led to the lowest value of wear loss, while the fifth one led to the maximum value of wear loss, as shown in Table 3.

4.2. Determination of optimum multiple performance for wear behavior

Experiments were done considering the planned L_{16} orthogonal array, the corresponding process responses of which are given in Table 4. According to the observations, with an increase in the SiC reinforcement from 3% to 6%, the frictional force and wear loss would be attenuated by 47.74% and 13.84%, respectively. With further increase in the silicon carbide to 9%, 1.91% increase in the frictional force and 16.66% decrease in

Table 3. L_{16}-experimental design.

Exp. no.	Input parameters				Output responses	
	SiC	Al_2O_3	Stirrer time (min)	Stirrer speed (rpm)	Wear loss (g)	FF (N)
1	3	2	5	500	0.021	10.30
2	3	4	10	600	0.006	13.20
3	3	6	15	700	0.015	7.60
4	3	8	20	800	0.014	26.33
5	6	2	10	700	0.025	7.20
6	6	4	5	800	0.012	24.67
7	6	6	20	500	0.011	4.00
8	6	8	15	600	0.007	3.00
9	9	2	15	800	0.017	15.23
10	9	4	20	700	0.013	11.55
11	9	6	5	600	0.016	7.55
12	9	8	10	500	0.020	5.30
13	12	2	20	600	0.022	6.88
14	12	4	15	500	0.008	8.22
15	12	6	10	800	0.019	14.55
16	12	8	5	700	0.018	20.52

Table 4. Normalizing, deviation sequence grey relation coefficient, and MRPI output response of AHMMCs.

Exp. no.	Normalizing sequence		Deviation sequence		Grey relational coefficient		Principal component		MRPI
	Wear loss (g)	FF (N)	Wear loss (g)	FF (N)	Wear loss (g)	FF (N)	Wear loss (g)	FF (N)	
1	0.211	0.687	0.789	0.313	0.388	0.615	0.194	0.307	0.501
2	1.000	0.563	0.000	0.437	1.000	0.534	0.500	0.267	0.767
3	0.526	0.803	0.474	0.197	0.514	0.717	0.257	0.358	0.615
4	0.579	0.000	0.421	1.000	0.543	0.333	0.271	0.167	0.438
5	0.000	0.820	1.000	0.180	0.333	0.735	0.167	0.368	0.534
6	0.684	0.071	0.316	0.929	0.613	0.350	0.306	0.175	0.481
7	0.737	0.957	0.263	0.043	0.655	0.921	0.327	0.460	0.788
8	0.947	1.000	0.053	0.000	0.905	1.000	0.452	0.500	0.952
9	0.421	0.476	0.579	0.524	0.463	0.488	0.232	0.244	0.476
10	0.632	0.634	0.368	0.366	0.576	0.577	0.288	0.288	0.576
11	0.474	0.805	0.526	0.195	0.487	0.719	0.244	0.360	0.603
12	0.263	0.901	0.737	0.099	0.404	0.835	0.202	0.418	0.620
13	0.158	0.834	0.842	0.166	0.373	0.750	0.186	0.375	0.561
14	0.895	0.776	0.105	0.224	0.826	0.691	0.413	0.345	0.758
15	0.316	0.505	0.684	0.495	0.422	0.502	0.211	0.251	0.462
16	0.368	0.249	0.632	0.751	0.442	0.400	0.221	0.200	0.421

the wear loss were observed. In the case of increasing the silicon carbide up to 12%, 21% increase in the frictional force and 1.49% wear loss were observed. In the case of Al_2O_3, reinforcement increased from 2% to 4%; frictional force increased up to 45.518%; and wear loss decreased by 117.94%. With further increase of Al_2O_3 to 6%, 84.5% decrease in the frictional force and 36.06% increase in the wear loss were observed. For Al_2O_3 of 8%, 38.98% increase in the frictional force and 3.389% decrease in the wear loss were observed. The stirrer time increased from 5 min to 10 min; frictional force decreased by 56.62%; and wear loss increased up to 4.285%. With further increase in the stirrer time up to 15 min, 30.98% and 3.98% decreases in the frictional force and wear loss, respectively, were observed. At the stirrer time of 20 min, with 30.16% increase in

Table 5. Eigen values and vector of principal components.

Components	Eigen value	Difference	Variation (%)	Cumulative (%)	Eigen vector (WL, FF)
Z_1 components	1.1599	0.3158	57.8	57.8	0.707, 0.707
Z_2 components	0.8441	—	42.2	100	0.707, –0.707

Table 6. Response table for multiresponse performance index.

Factor	Level-1	Level-2	Level-3	Level-4	Max-Min	Rank
Sic	0.5802	0.6888	0.5686	0.5506	0.1382	3
Al_2O_3	0.5181	0.6456	0.6171	0.6076	0.1275	4
Stirrer time (min)	0.5016	0.5956	0.7003	0.5908	0.1987	2
Stirrer speed (rpm)	0.6667	0.7208	0.5365	0.4643	0.2565	1

the frictional force, 14.28% wear loss was observed. If the stirrer speed increased from 500 rpm to 600 rpm, the frictional force would increase up to 9.17% and wear loss would decrease by 17.64%. With further increase in the stirrer speed up to 700 rpm, 25.13% and 28.16% rates of increase in the frictional force and wear loss, respectively, were observed. At a stirrer speed of 800 rpm, upon increasing the frictional force up to 41.978%, wear loss would decrease by 1.91%.

The outputs are normalized by using Eq. (1) and the case considered as lower the better. Table 4 lists the GRA measured experimental values. Next, Eq. (2) is used to measure the GRC. Followed by calculating the GRC, the multiresponse outputs in the PC analysis method given in Table 4 are measured.

As determined by the PCA, the eigenvectors for frictional force and wear loss are 0.707 and 0.707 for eigenvalues of 1.159, respectively, because an eigenvalue greater than one is necessary. These values are shown in Table 5.

Table 6 represents the Multi Response Performance Index (MRPI) calculated with an optimum level of parameters. The optimum parameter levels were identified as 6% SiC, 4% Al_2O_3, stirrer time of 15 min, and stirrer speed of 600 rpm. Considering the average MRPI, Figure 3 illustrates the main effects plot.

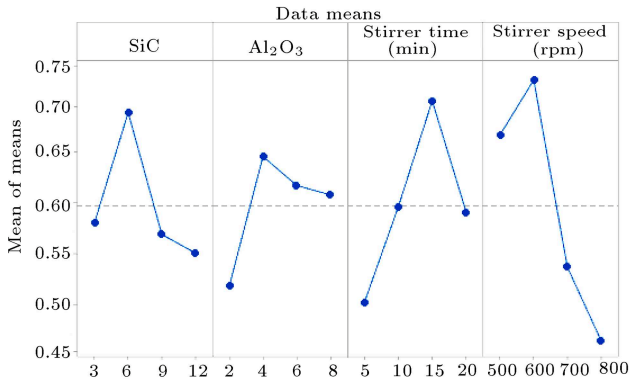

Figure 3. Main effect plot for multiresponse performance index.

The interaction plot is illustrated in Figure 4 according to which the parallel plot lines for all values can be identified, and there is no significant interaction between the stirrer speed and other parameters. However, there is a significant variable interaction between the values of aluminum oxide and stirrer time as well as the values of aluminum oxide and silicon carbide at all selected levels. In addition, a considerable interaction occurs between the stirrer time and silicon carbide and apparently, there is a non-parallel line relationship between them [24].

4.2.1. Analysis of Variance (ANOVA)

Analysis of Variance (ANOVA) was employed in this study to measure the extent of process development. It was also used to identify the determining parameters and interpret the experimental data from experimental responses. In addition, Minitab-19 was used in the optimization process.

A statistical method namely ANOVA was applied to evaluate the effects of the categorical parameters on an output response [25]. The difference in the output response is decomposed by ANOVA between the different input factors. To evaluate the most contributing parameter to the output responses, the ANOVA table is generated. Table 7 shows the MRPI results obtained from ANOVA. The stirrer speed is the most significant parameter whose contribution percentage to the output responses was obtained as 49.40% followed by that of the stirrer time, i.e., 23.61%. According to the findings, 2.23% error value indicated that the obtained values were sufficient enough to performed the process analysis. The obtained R^2 value and $R^2(adj)$ values were measured as 97.77% and 88.85%, respectively.

4.2.2. Confirmation experiment results

A process confirmation experiment evaluates the PCA-GRA technique's chosen parameters to see how well they work. The optimum input parameters for this investigation were 6% silicon carbide, 4% aluminum oxide, 15 minutes of stirring, and a 60 rpm stirrer

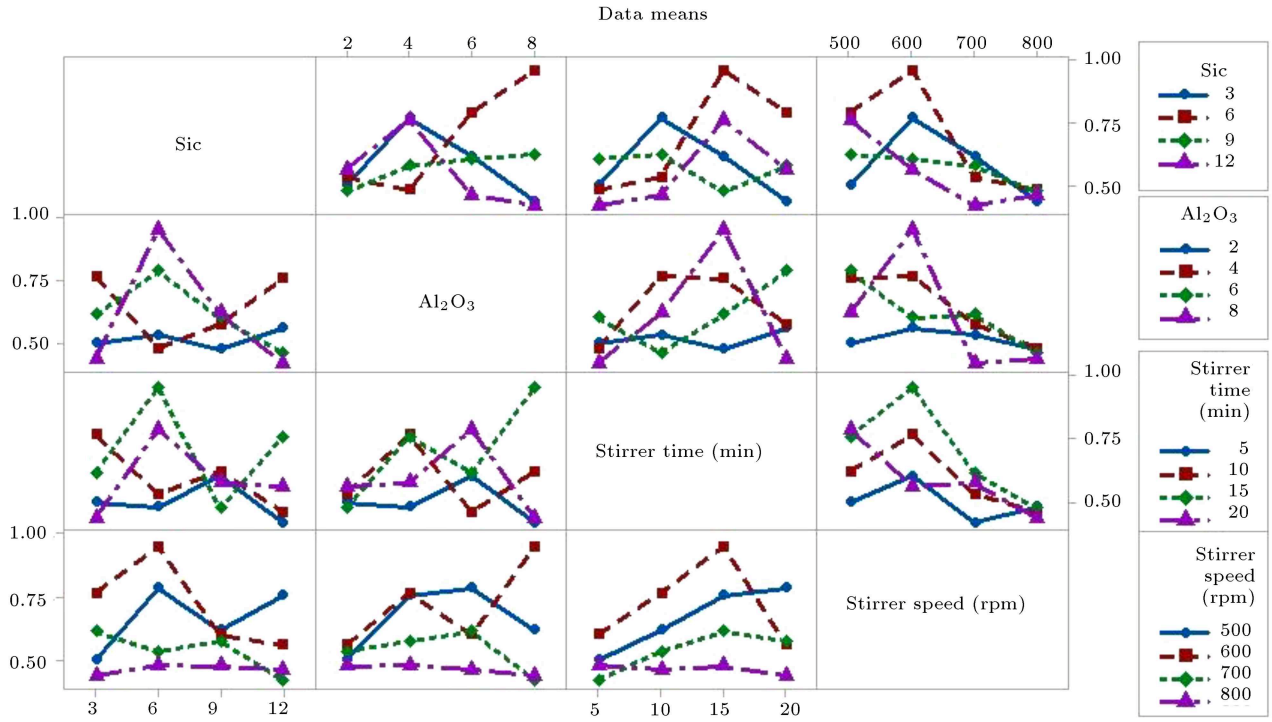

Figure 4. Interaction plot for multiresponse performance index.

Table 7. Analysis of variance for multiresponse performance index.

Source	DF	Seq SS	Adj SS	Adj Ms	*F*-value	*P*-value	Contribution
Sic	3	0.046694	0.046694	0.015565	6.24	0.083	13.91%
Al_2O_3	3	0.036402	0.036402	0.012123	4.87	0.113	10.85%
Stirrer time (min)	3	0.079257	0.079257	0.026419	10.59	0.042	23.61%
Stirrer speed (rpm)	3	0.165801	0.165801	0.055267	22.16	0.015	49.40%
Error	3	0.007482	0.007482	0.002494	—	—	2.23%
Total	15	0.335636	0.335636	—	—	—	100.00%

speed, which resulted in a frictional force of 1.4 N and a wear loss of 0.0034 g. The improvement in average frictional force and wear loss was reported to be 52.63% and 42.85%, respectively. The specimen fabricated with optimum parameters was characterized by the mechanical characteristics namely the micro hardness of 154.22 BHN, tensile strength of 443.61 MPa, and impact strength of 3 J.

4.2.3. CI calculation

Confidence Interval (CI) is defined as determination of the interval estimation for the given population parameter that limits the population or distribution parameters. The CI length determines the estimation accuracy and that an accurate calculation has short intervals [26]. CI value was determined to verify the confirmation results for which the approximate mean of final MRPI was calculated from the optimal results as $A_2B_2C_3D_2$:

$$MRPIem = SiC_2 + Al_2O_3 + ST_3 + SS_2, \quad (9)$$

where $MRPIem$ represents estimated mean of MRPI, SiC_{2m}-Mean MRPI of silicon carbide, Al_2O_{3m}-Mean MRPI of aluminium oxide, ST_{3m}-Mean MRPI of stirrer time, and SS_{2m} -Mean MRPI of stirrer speed. In order to evaluate the estimated MRPI, the mean value of the above optimal parameter levels should be determined and substituted into Eq. (9):

$$MRPIem = 06888 + 0.6456 + 0.7003 + 0.7208 - (3^*0.597) = 0.964.$$

Based on the confirmation experiments, CI is calculated below to predict the mean of MRPI:

$$CI = \sqrt{f_{0.05}(3, f_e)v_e\left[\frac{1}{n} + \frac{1}{R}\right]}, \quad (10)$$

where f_e is the error degrees of freedom (Eq. (3))

from the ANOVA shown in Table 7; $f_{0.05}(3, f_e)$ is f ratio for $(3,3) = 9.28$ taken from fisher table in standard value; v_e is the error (0.002494) from the ANOVA shown in Table 7; R is the number of replications of confirmation, i.e., $Exp. - 1$; N is the total number of experiments performed by $n_r \times$ number of experiments $= 1 \times 16 = 16$ where n_r is the number of repetitions/replications (Eq. (3)); and n is the effective number of replications obtained by $N/(1+\text{DOF})$ which associated with MRPI shown in Table 7 is equal to $16/(1+15) = 1$.

The CI value for MRPI is determined based on the above relations as follows:

$$CI = \{9.28 \times 0.002494[(1/1)+(1/1)]^{1/2} = 0.215. \quad (11)$$

The 95% confidence CI of the optimal confirmation experiment-based MRPI is:

$$(MRPI - CI) < MRPI_{con} < (MRPI + CI). \quad (12)$$

The results of the confirmation experiment prove that the given MRPI falls in between $(MRPIem - CI)$ and $(MRPIem + CI)$. (i.e., 0.957 falls between 0.749 and 1.179). In this regard, the validated MRPI is verified through Eq. (11).

4.3. Mechanical characterization

According to the OA of L_{16}, the procedure was performed for 16 different castings. The cast parts were machined based on the ASTM standards. In Vicker's ASTM E384 micro hardness tester, the hardness test was done considering the information provided in Figure 5. Here, a load of 0.5 kg was applied to the specimens at the time of 10 seconds. According to ASTM B557M (Figure 6), the tensile test rod was machined and the testing was done on a computer-based controlled fine universal tension unit at a steady speed of 1 mm/min at ambient temperature. The impact testing machine (Figure 7) was used to test the impact strength value of the AHMMCs and according to the findings, Charpy impact tests followed the ASTM E24 standard. The sample density was determined, considering the high accuracy of the digital electronic system based on Archimedes' principle and porosity tests carried out in ASTM E2109. Table 8 lists all conducted tests at room temperature [27–29].

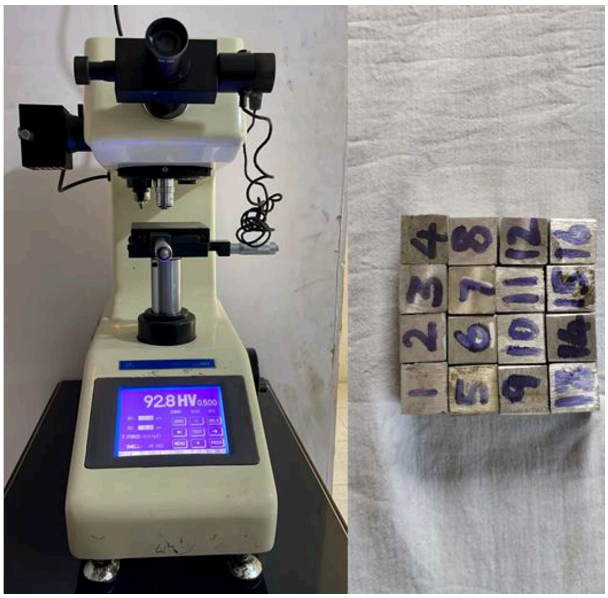

Figure 5. Hardness tester setup.

4.3.1. Wear surface morphology

The SEM analysis identified a worn-away surface of AHMMCs pins, followed by the wear testing, as shown in Figure 8(a) and (b), respectively. In Figure 8(a), the deep groove form represents the wear track, debris, and ploughing as marked and defined. It shows the removed material through ploughing. The interface region temperature is increased by these particles, resulting in the loss of material wear resistance. Due to an increase in the surface temperature, the longer running time of produced heat results in the AHMMCs softening. In Figure 8(b), it is shown that the wear track of material is noted along the sliding path. It does not generate any wear debris, but surfaces are conditioned properly. This means that the lowest temperature is produced properly and dissipated in the interface field, which occurs at the lower running time [30]. The action of deep grooves has been visible. These grooves were created due to plastic flow for composite material, induced by the appearance of hard silicon carbide reinforcement agents due to the cutting effect [31]. Similarly, while decreasing the size of the grain and contact load, the wear scratch is decreased and it is noted that stiffness, rigidity and fracture toughness are increased [32]. Usually, the condition of mild wear produced abrasion wear [33].

4.4. Energy dispersive spectrum analysis of AHMMCs

EDX analysis evaluates the asperity activity relationship between two touching surfaces, as shown in Figure 9(a) and (b). On the worn-away surface layer of the test material, the presence of C, O, mg, Al, Fe, Cu, and Zn elements can be confirmed (Figure 9(a)). The combined layer in this figure was formed as a result of the transfer of Fe from the high C and high Cr steel disk to the composite as well as the removal of surface specimen in aluminum. This layer will protect the composite only in the region of intermediate temperature and load. Figure 9(b) shows the EDX analysis of lower wear loss specimen. The impact of oxygen and aluminum oxide in the debris would be attenuated due to higher frictional heating, thus resulting in the increased sliding surface temperature. This

Figure 6. Tensile test setup and specimens.

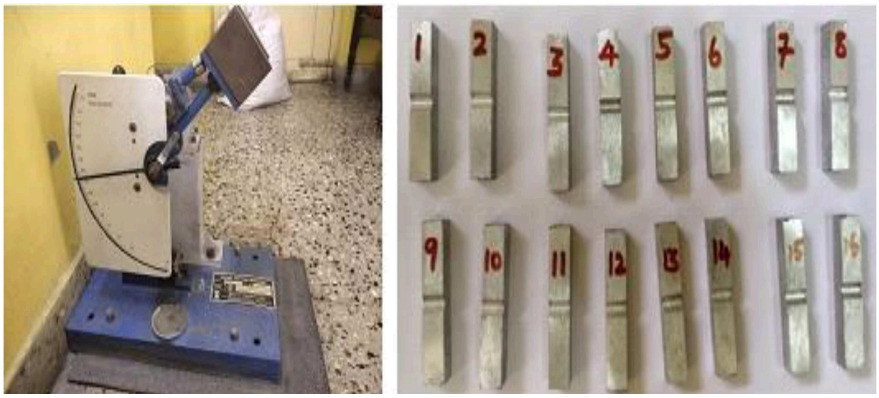

Figure 7. Impact test setup and specimens.

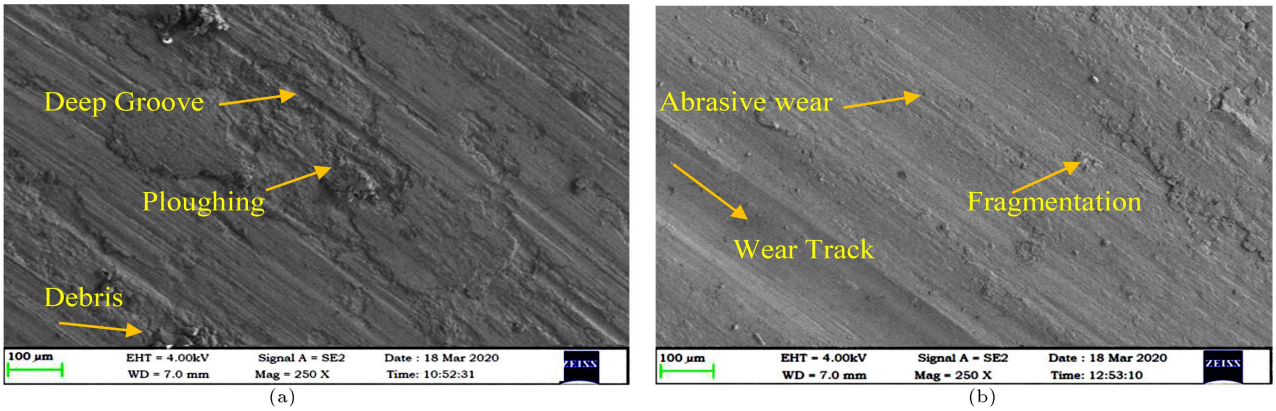

(a) (b)

Figure 8. SEM morphology: (a) Higher wear loss specimen and (b) lower wear loss specimen.

Table 8. Mechanical properties of AHMMCs.

Trail no.	Tensile strength (MPa)	Hardness (BHN)	Impact value (J)	Density (g/cm^3)	Porosity (%)
1	376.436	130.91	5.2	2.72	1.01
2	415.575	149.56	3.57	2.75	0.85
3	396.714	138.21	5.94	2.73	1.08
4	406.853	141.86	6.31	2.74	1.11
5	298.946	92.358	9.53	2.76	2.1
6	334.893	114.33	9.02	2.77	1.44
7	409.872	142.688	3.63	2.79	1.26
8	413.82	146.66	4.15	2.81	0.97
9	300.118	96.064	11.29	2.8	2.32
10	339.581	112.229	8.6	2.83	2.08
11	366.661	129.038	6.21	2.84	1.2
12	406.124	145.203	3.52	2.85	1.1
13	313.276	105.542	8.98	2.86	2.5
14	346.548	117.029	6.44	2.87	1.95
15	321.171	108.486	10.02	2.89	1.92
16	354.442	124.973	7.48	2.88	1.36

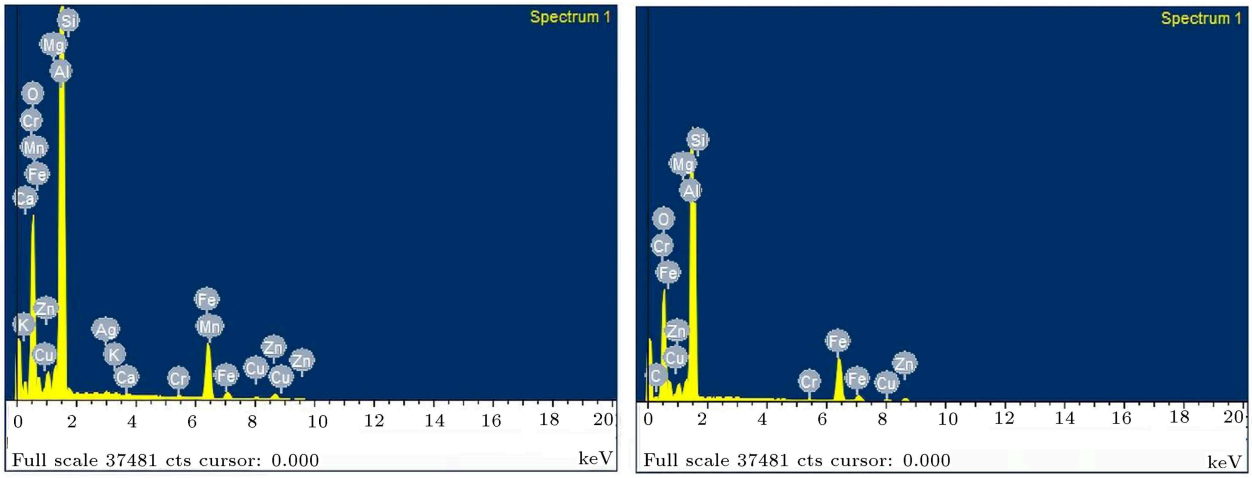

(a) (b)

Figure 9. EDX analysis: (a) Higher wear loss specimen and (b) lower wear loss specimen.

EDX image also shows the delimited debris surface that is responsible for improving the composite wear properties [34].

5. Conclusions

PCA-GRA technique was employed in this study to optimize the conditions of the stir casting process for Al7075 ($SiC+Al_2O_3$). From the experimental results, the following conclusions are drawn:

- The experimental results indicated that the optimal wear loss and frictional force could be achieved by incorporating 6% SiC and 4% Al_2O_3 at the stirrer time and speed of 15 min and 600 rpm, respectively;
- According to the results from ANOVA, the contribution share of the stirrer speed as the filler effect of the material towards the output was 49.40%, while the values of the stirrer time, SiC, and Al_2O_3 were 23.61%, 13.91%, and 10.85%, respectively;
- According to the confirmation wear test done on the optimized input parameters, there was a 42.85% increase in the wear resistance as well as a 52.63% increase in the frictional force, thus confirming the experimental results;
- From the Scanning Electron Microscope (SEM) and Energy Dispersive X-ray (EDX) analyses, changes in the internal structure during wear tests were confirmed through the SEM images, wear track, grooves, debris, and ploughings. The EDX analysis explains the asperity behavior between two mating surfaces.

Acknowledgment

The authors wish to express their grateful thanks to the Department of Mechanical engineering, Arunai Engineering College, Thiruvannamalai, Tamilnadu, India for supporting this research work.

Nomenclature

Al_2O_3	Aluminum Oxide
ANOVA	Analysis of Variance
AHMMCs	Aluminum Hybrid Metal Matrix Composites
CI	Confidence Interval
DoE	Design of Experiments
EDX	Energy Dispersive X-ray analysis
FF	Frictional Force
GRA	Grey Relational Analysis
MRPI	Multi Response Performance Index
PCA	Principal Component Analysis
POD	Pin-On-Disc
SiC	Silicon Carbide
SEM	Scanning Electron Microscope

References

1. An, Q., Chen, J., Ming, W., et al. "Machining of SiC ceramic matrix composites: A review", *Chinese Journal of Aeronautics*, **34**, pp. 540–567 (2021).
2. Siddabathula, M., Mohammed Moulana, M., et al. "Mechanical properties of Aluminum-Copper composite metallic materials", *Journal of Applied Research and Technology*, **14**, pp. 293–299 (2016).
3. Chen, J., Yu, W., Zuo, Z., et al. "Effects of in-situ TiB_2 particles on machinability and surface integrity in milling of TiB_2/2024 and TiB_2/7075 Al composites", *Chinese Journal of Aeronautics*, **34**, pp. 110–124 (2021).

4. Devaganesh, S., Dinesh Kumar, P.K., Venkatesh, N., et al. "Study on the mechanical and tribological performance of hybrid SiC-7075 metal matrix composites", *Journal of Materials Research and Technology*, **9**, pp. 3759–3766 (2020).

5. Malekjafariana, M. and Sadrnezhaad, S.K. "Effect of SiC on microstructural features and compressive properties of aluminum foam", *Scientia Iranica*, **21**, pp. 1325–1329 (2014).

6. Ehsani, R. "Aging behavior and tensile properties of squeeze cast Al 6061/SIC metal matrix composites", *Scientia Iranica*, **29**, pp. 864–882 (2022).

7. Rino, J.J., Chandramohan, D., Sucitharan, K.S., et al. "An overview on development of aluminium metal matrix composites with hybrid reinforcement", *IJSR*, **1**, pp. 196–203 (2012).

8. Ravichandrana, M., Meignanamoorthy, M., Chellasivam, G.P., et al. "Effect of stir casting parameters on properties of cast metal matrix composite", *Materials Today: Proceedings*, **22**, pp. 2606–2613 (2020).

9. Alaneme, K.K. and Bodunrin, M.O. "Corrosion behavior of alumina reinforced aluminium (6063) metal matrix composites", *Journal of Minerals and Materials Characterization and Engineering*, **12**, pp. 1153–1165 (2011).

10. Balaji, V., Sateesh, N., Manzoor Hussian, M. "Manufacture of aliminium metal matrix composite (Al7075-SiC) by stir casting technique", *Material Today Proceedings*, **2**, pp. 3403-3408 (2015).

11. Das, P.P. and Chakraborty, S. "Application of grey correlation-based EDAS method for parametric optimization of non-traditional machining processes", *Scientia Iranica*, **29**, pp. 864–882 (2022).

12. Thirumalvalavan, S. and Senthilkumar, N. "Optimising the wear performance of HVOF thermal spray coated Ti-6Al-4V alloy by grey relational approach", *International Journal of Rapid Manufacturing*, **9**, pp. 25–47 (2020).

13. Devaraju, A., Kumar, A., and Kotiveerachari, B. "Influence of rotational speed and reinforcements on wear and mechanical properties of aluminum hybrid composites via friction stir processing", *Materials and Design*, **45**, pp. 576–585 (2013).

14. Samal, P., Vundavilli, P., et al. "Recent progress in aluminum metal matric composites: A review on processing, mechanical and wear properties", *Journal of Manufacturing Processes*, **59**, pp. 131–152 (2020).

15. Samiee, A. and Meratian, M. "Influence of alumina percentage on hot deformation of aluminium–alumina matrix composite", *International Journal of Cast Metals Research*, **28**, pp. 47–49 (2014).

16. Taguchi, G., *Introduction to Quality Engineering*, Asian Productivity Organization (1990).

17. Asima, M., Zubair Khanb, M., Alam Khan, L., et al. "An integrated approach of quality for polymer composite manufacturing validated and optimized through Taguchi method", *Scientia Iranica*, **24**, pp. 1985–1995 (2017).

18. Senthilkumar, N., Tamizharasan, T., and Anandakrishnan, V. "Experimental investigation and performance analysis of cemented carbide inserts of different geometries using Taguchi based grey relational analysis", *Measurement*, **58**, pp. 520–536 (2014).

19. Ghosh, S., Sahoo, P., and Sutradhar, G. "Wear behaviour of Al-SiCp metal matrix composites and optimization using Taguchi method and grey relational analysis", *Journal of Minerals and Materials Characterization and Engineering*, **11**, pp. 1085–1094 (2012).

20. Hotelling, H. "Analysis of a complex of statistical variables into principal components", *Journal of Educational Psychology*, **24**, pp. 417–441 (1993).

21. Pearson, K. "LIII. On lines and planes of closest fit to systems of points in space", *The London, Edinburgh, and Dublin Philosophical Magazine and Journal of Science*, **11**, pp. 559–572 (1901).

22. Rajesh, S., Gopala Krishna, A., Rama Murty Raju, P., et al. "Statistical analysis of dry sliding wear behavior of graphite reinforced aluminum MMCs", *Procedia Materials Science*, **6**, pp. 1110–1120 (2014).

23. Kumar, M., MegalingamMurugan, A., Baskaran, V., et al. "Effect of sliding distance on dry sliding tribological behaviour of aluminium hybrid metal matrix composite (AlHMMC): An alternate for automobile brakerotor – A Grey relational approach", *Journal of Engineering Tribology*, **230**, pp. 1–14 (2016).

24. Senthilkumar, N. and Tamizharasan, T. "Effect of tool geometry in turning AISI 1045 steel: Experimental investigation and FEM analysis", *Arabian Journal for Science and Engineering*, **39**, pp. 4963–4975 (2014).

25. Gamst, G., Meyers, L.S., and Guarino, A.J., *Analysis of Variance Designs - A Conceptual and Computational Approach with SPSS and SAS Cambridge University Press*, Cambridge UK (2008).

26. Montgomery, D.C., *Design and Analysis of Experiments*, Eight Ed., John Wiley & Sons, Inc., USA (2013).

27. Ravi Kumar, K., Kiran, K., and Sreebalaji, V.S. "Microstructural characteristics and mechanical behaviour of aluminium matrix composites reinforced with titanium carbide", *Journal of Alloys and Compounds*, **723**, pp. 795–801 (2017).

28. Suvarna Raju, L. and Kumar, A. "Influence of Al_2O_3 particles on the microstructure and mechanical properties of copper surface composites fabricated by friction stir processing", *Defence Technology*, **10**, pp. 375–383 (2014).

29. Soorya Prakash, K., Gopal, P.M., Anburose, D., et al. "Mechanical, corrosion and wear characteristics of powder metallurgy processed Ti-6Al-4V/B4C metal matrix composites", *Ain Shams Engineering Journal*, **9**, pp. 1489–1496 (2018).

30. Kaushik, N. and Singhal, S. "Optimization of wear properties in aluminum metal matrix composites using hybrid Taguchi-GRA-PCA", *International Journal of Performability Engineering*, **14**, pp. 857–870 (2018).

31. Jeyasimman, D., Narayanasamy, R., Ponalagusamy, R., et al. "The effects of various reinforcements on dry sliding wear behaviour of AA 6061 nanocomposites", *Materials & Design*, **64**, pp. 783–793 (2014).

32. Jayakumar, L. and Balamurugan, K. "Reciprocating wear behavior of 7075Al/SiC in comparison with 6061Al/Al_2O_3 composites", *Int. Journal of Refractory Metals and Hard Materials*, **46**, pp. 137–144 (2014).

33. Singh, R., Shadab, M., Dash, A., et al. "Characterization of dry sliding wear mechanisms of AA5083/B4C metal matrix composite", *Journal of the Brazilian Society of Mechanical Sciences and Engineering*, **41**, pp. 1–11 (2019).

34. Edidiong, D.A., Alastair, M., et al. "Evaluation of Cd(II) ion removal from aqueous solution by a low-cost adsorbent prepared from white yam (dioscorea rotundata)waste using batch sorption", *ChemEngineering*, **2**, pp. 1–36 (2018).

Biographies

Saminathan Selvarasu is an Assistant Professor in Mechanical Engineering at Arunai Engineering College in India. His research interests include composite materials and design of experiments. He has published several papers concerning composite materials in some accredited international journals such as Thermal Science International Scientific Journal, and Silicon, to name a few. He is currently working on the performance characterization of CI engines equipped with composite piston.

Lakshmipathy Jayakumar is a Professor and the Head Deputy of Mechanical Engineering at Arunai Engineering College, Tiruvannamalai, Tamilnadu, India. He holds BE, ME, and PhD degrees in Mechanical Engineering from Bharathiyar University, Anna University, and Anna University Chennai, respectively. He is a recognized supervisor at Anna University, Chennai. His research interests are composite materials, vibration analysis, and optimization. He has published many papers on the composite materials in some high ranking international journals such as International Journal of Refractory metals and Hard Materials, Science and Engineering of Composite Materials, Journal of Vibration and Control, Iranian Journal of Science and Technology, Transactions of Mechanical Engineering, etc. Under his supervision, two scholars could complete their doctoral program.